DENSITY FUNCTIONAL THEORY CALCULATIONS AND *IN SILICO* STUDIES ON THE SCHIFF BASE DERIVATIVES WITH ANTIBACTERIAL ACTIVITIES

HELEN P KAVITHA[1]*, ARTHI P[1], ARULMURUGAN S[1], KAVIPRIYA R[1], JASMINE P VENNILA[2]

[1]Department of Chemistry, SRM Institute of Science and Technology, Chennai, Tamil Nadu, India. [2]Department of Physics, Panimalar Institute of Technology, Chennai, Tamil Nadu, India. Email: helenkavitha1971@gmail.com

ABSTRACT

Objective: Heterocyclic compounds play a key role in biological processes and are wide spread as natural products. In this research, we have mainly focused on the investigation of heterocyclic Schiff base compounds.

Methods: The heterocyclic Schiff bases *(N^1Z,N^4Z)-N^1,N^4-bis(3,4-methoxyphenyl)methylidene) benzene-1,4-diamine* **(1)**, (N^1Z,N^4Z)-$N^1,N4$-bis (4-bromobenzylidene)benzene-1,4-diamine **(2)**, and *(N^1Z,N^4Z)-N^1,N^4-bis(furan-2-ylmethyliden)benzene-1,4-diamine* **(3)** were synthesized and characterized by Fourier-transform infra-red spectroscopy and proton nuclear magnetic resonance spectroscopy. The bond length, bond angle, and highest occupied molecular orbital–lowest unoccupied molecular orbital energy gap were calculated out by density functional theory (DFT) calculations. The synthesized heterocyclic compounds **(1-3)** were screened for their antibacterial activity against *Staphylococcus aureus* and *Escherichia coli*.

Results and Discussion: As a result of our research, the compound **3** displays superior antibacterial activity compared to standard drug Streptomycin. All the compounds significantly interact with antibacterial protein beta-ketoacyl-acp synthase III and anticancer protein c-Kit tyrosine kinase through π–π, σ–π, hydrogen bonding, electrostatic, and Van der Waals interactions.

Conclusion: The molecular docking results showed that the compounds strongly interact with both antibacterial and anticancer receptor protein and give better free energy of bindings.

Keywords: Heterocyclic Schiff bases, Density functional theory calculations, Antibacterial, *In silico* studies.

INTRODUCTION

Heterocyclic compounds are organic compounds containing at least one atom of carbon and at least one element other than carbon, such as sulfur, oxygen, or nitrogen within a ring structure [1]. In heterocycles, non-carbons are considered to replace carbon atoms and are called heteroatoms, for example, different from carbon and hydrogen. A ring with only heteroatoms is called homocyclic compound and heterocycles are the counterparts of homocyclic compounds. These structures may comprise either simple aromatic rings or non-aromatic rings. The heterocyclic compounds usually possess a stable ring structure which does not readily hydrolyzed or depolymerized. Heterocycles with three atoms in the ring are more reactive due to ring strain. Those containing one heteroatom are in general, stable. Those with two heteroatoms are more likely to occur as reactive intermediates.

Heterocyclic compounds play a key role in biological processes and are widespread as natural products. They are widely found in nature particularly in nucleic acids, plant alkaloids, anthocyanins, and flavones as well as in heme and chlorophyll. In addition, some vitamins, proteins, and hormones contain the aromatic heterocyclic system. Synthetically produced heterocycles designed by organic chemists are used for instance as agrochemicals and pharmaceuticals and play an important role in human life. Heterocycles have enormous potential as the most promising molecules as lead structures for the design of new drugs [2].

Schiff bases are condensation products of primary amines with carbonyl compounds and they were first reported by Schiff [3] in 1864. The common structural feature of these compounds is the azomethine group with a general formula RHC=N–R1, where R and R1 are alkyl, aryl, cycloalkyl or heterocyclic groups, which may be variously substituted [4-8].

Herein, we report density functional theory (DFT) studies on the Schiff base compounds synthesized by the condensation of 3,4-dimethoxybenzaldehyde, 4-bromobenzaldehyde, and furfuraldehyde with *p*-phenylenediamine. The biological efficacy of the compounds was tested in terms of antibacterial activity. Further, an in-depth theoretical understanding of Mulliken charges, nonlinear optical (NLO), highest occupied molecular orbital–lowest unoccupied molecular orbital (HOMO–LUMO), molecular electrostatic potential (MESP), dipole moment, linear polarizability, and first hyperpolarizability calculations were carried out using the Gaussian 03 program. The synthesized compounds have also been evaluated for their ability to inhibit the antibacterial and anticancer proteins.

EXPERIMENTAL SECTION

Materials and instrumentation

All chemicals were analytical grade and used without further purification. Solvents used for spectroscopic studies were HPLC grade. 3,4-dimethoxybenzaldehyde, and 4–bromobenzaldehyde and furfuraldehyde was purchased from E. Merck and Sigma-Aldrich, respectively. Proton nuclear magnetic resonance (^{1}H NMR) spectral data were obtained on Varian-VNMRS-400 in CDCl$_3$ and dimethyl sulfoxide (DMSO) solution with tetramethylsilane as an internal standard at ambient temperature. Fourier-transform infrared spectra were recorded on ABB instruments, MB-3000 spectrophotometer using KBr pellets in the range of 4000–400 cm^{-1}.

Synthesis of Schiff base compounds [9,10]

(N^{1}Z,N^{4}Z)-N^1,N^4-bis(3,4 methoxyphenyl methylidene)benzene-1, 4-diamine (1)

About 1.08 g (0.01 mol) of *p*-phenylenediamine and 1.66 g (0.01 mol) of 3,4-dimethoxybenzaldehyde were taken in a 250 ml R.B flask. 40 ml of ethanol was added into the flask slowly and the mixture was refluxed for 5 h. It was then allowed to cool and filtered. The compound was recrystallized from ethanol.

Yield: 72%. Color: Yellow. M. P: 185°C. Selected IR (KBr) (ν/cm^{-1}): 2924.23 ν(O–CH$_3$), 3011.86 ν(Ar–CH), 1617.62 ν(C=N). ^{1}H NMR (δ/ppm in CDCl$_3$): 6.93–7.31 (d, 3H, CH3 protons), 6.68–6.70 (Benzylic-H).

(N^{1}Z,N^{4}Z)-N^1,N^4(4 bromophenyl methylidene)benzene -1,4-diamine (2)

This compound was obtained by following the procedure similar to that for **1**, using 4-bromobenzaldehyde in place of 3,4-dimethoxybenzaldehyde.

Yield: 68 %. Color: Yellow. M. P: 130°C. Selected IR (KBr) (ν/cm^{-1}): 1610.61 ν(C=N), 2919.40, ν(Ar–CH), 514.44 ν(–Br). ^{1}H NMR (δ/ppm in CDCl$_3$): 7.15–7.16 (d, Ar-H), 6.86–6.96 (Benzylic-H).

(N^{1}Z,N^{4}Z)-N^1,N^4-bis(furan-2-ylmethylien)benzene -1,4 diamine (3)

This compound was obtained by following the procedure similar to that for **1**, using furfuraldehyde in place of 3,4-dimethoxybenzaldehyde.

Yield: 70 %. Color: Yellow. M. P: 134°C. Selected IR (KBr) (ν/cm^{-1}): 1621.45 ν(C=N), 3024.06 ν(Ar–CH), 1275.24, ν(C–O). ^{1}H NMR (δ/ppm in CDCl$_3$): 7.17–7.29 (d, Ar–H), 6.86–6.96 (Benzylic-H).

Quantum chemical calculations

The quantum chemical calculations are performed at B3LYP/6-311G(d) basis sets using the Gaussian 03W program. The optimized structural parameters are evaluated for the calculations of vibrational frequencies by assuming C$_s$ point group symmetry. At the optimized geometry for the title molecules no imaginary frequency modes were obtained; therefore, minimum on the potential energy surface was found. As a result, the unscaled calculated frequencies and infrared intensities are obtained. GaussView program [11] is considered to get visual animation and for the verification of the normal modes assignment.

Antibacterial activity

The compounds (**1-3**) were tested against two different microorganisms such as *Staphylococcus aureus* and *Escherichia coli*. The agar well-diffusion method [12] is applied for the determination of the inhibition zone. Briefly, 0.75 mL of broth culture containing *ca.* 106 colony-forming units per mL of the test strain was added to 75 mL of nutrient agar medium at 45°C, mixed well and then poured into a 15 cm sterile metallic Petri plate. The medium was allowed to solidify and 8 mm wells were dug with a sterile metallic borer. Then, absolute ethanol solution of the test sample (1 mL) at 1 mg/mL was added to the respective wells. Streptomycin served as control. The plates for each strain were prepared and were incubated aerobically at 37°C for 24 h. The activity was determined by measuring the diameter of zone showing complete inhibition (mm); thereby, the zones were precisely measured with the aid of a Vernier caliper (precision 0.1 mm).

Molecular docking studies

Ligand preparation

Docking calculations were carried out using the docking server [13]. The MMFF94 force field [14] was used for energy minimization of ligand molecules using docking server. Gasteiger partial charges were added to the ligand atoms. Non-polar hydrogen atoms were merged and rotatable bonds were defined.

Protein preparation

The X-ray crystal structure of tide antimicrobial beta-ketoacyl-acp synthase III+ malonyl-CoA receptor (PDB: 1HNJ) and anticancer protein c-Kit tyrosine kinase (PDB: 1T46) protein obtained from the protein data bank. Essential hydrogen atoms, Kollman united atom type charges and solvation parameters were added with the aid of AutoDock tools [15]. Affinity (grid) maps of 20 × 20 × 20 Å grid points and 0.375 Å spacing were generated using the Autogrid program.
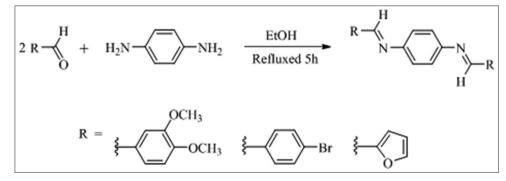
Computational methods

Docking simulations were performed using the Lamarckian genetic algorithm, and the Solis and Wets local search method [16]. Initial position, orientation, and torsions of the ligand molecules were set randomly. Each docking experiment was derived from 10 different runs that were set to terminate after a maximum of 250,000 energy evaluations. The population size was set to 150. During the search, a translational step of 0.2 Å and quaternion and torsion steps of 5 were applied.

RESULTS AND DISCUSSION

The synthesized heteroleptic Schiff base compounds (**1-3**) have been isolated using general procedure and obtained in good yield (Scheme 1). They are non-hygroscopic in nature. The yellowish compounds are soluble in most of the organic solvents. The authenticities of compounds were ascertained by FT-IR and ^{1}H NMR spectra.

Spectral characterization

FT IR spectra of Schiff base compounds (**1-3**) framework are confirmed by the absence of bands characteristic of starting materials: The band due to aldehydic –C=O band at 1680 cm^{-1} disappeared and band for imine stretching appear as sharp band in the region 1610–1621 cm^{-1} (**1-3**) [17,18], no peaks attributed to NH$_2$ groups implied that the effective Schiff's base condensation reaction has been completed. A strong absorption band around 1275, 513, and 2924 cm^{-1} corresponding to C–O, C–Br, and O–CH$_3$ stretching vibrations. The bands at 3024 cm^{-1} were assigned to aromatic –CH vibrations of the compounds.

Scheme 1: Synthesis of Schiff base heterocyclic compound (1-3)

The ^{1}H NMR spectra of compounds were recorded in DMSO-D$_6$ show well-resolved signals as expected (Fig. 1). The compound 1 shows that three doublets at δ 7.29–7.31, 7.11–7.13, and 6.91–6.93 are attributed to Ha, Hb, and Hc protons of the phenyl ring carrying methoxy group, respectively. In compound **2** a doublet observed at δ 7.17–7.29 may be assigned to the aromatic protons of the benzene ring of *p*-phenylenediamine. A doublet observed at δ 6.70–6.72 and 7.15–7.16 may be assigned to the aromatic protons of the benzene ring of *p*-phenylenediamine. Two doublets observed at δ 7.73–7.75 and 7.93–7.95 are attributed to Ha and Hb protons of the phenyl ring, respectively.

A aromatic protons observed at δ 6.70–7.29 ppm, the furan ring protons at δ 6.56–7.61 ppm. A singlet observed at δ 8.32 in the proton NMR spectrum of the compound **3** confirms the presence of azomethine group in the compound. Three doublets observed at δ 6.56–6.59, 6.86–6.96, and 7.29–7.61 are attributed to Ha, Hb, and Hc protons of the furan ring, respectively.

Computational studies

MESP

MESP provides a visual method to understand the relative polarity of the molecule [19]. The different values of the electrostatic potential at the surface are represented by different colors. Potential increases in the order red < orange < yellow < green < blue. Red regions indicate regions of most negative electrostatic potential, blue regions indicate regions of most positive electrostatic potential, and green region represents region of zero potential. Such mapped electrostatic potential surface has been plotted for the title compounds using GaussView 03 employing 6-31G(d) basis set. The MESP map shows that the negative regions (red) are over the nitrogen atoms; hence, electrophilic attack can take place in these sites. The positive regions (blue) are over the hydrogen atoms of the title compounds; hence, nucleophilic attack can take place in these regions. Thus, MESP map has been used primarily to identify electrophilic and nucleophilic sites and in studies of biological recognition and hydrogen bonding interactions [20]. Figs. 2
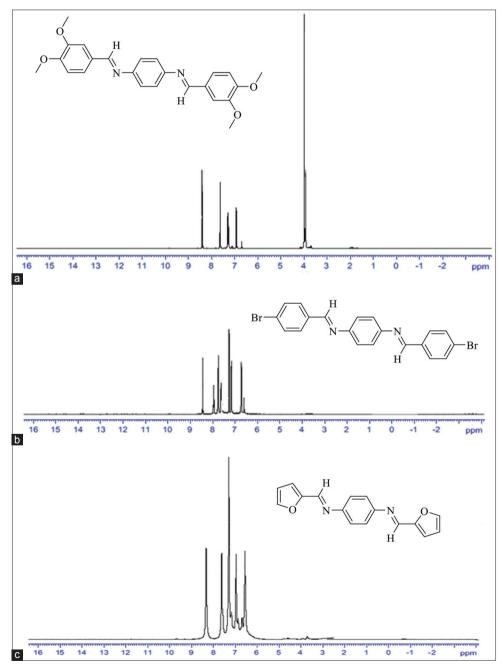

Fig. 1: Proton nuclear magnetic resonance spectra of compounds 1 (a), 2 (b), and 3 (c)

and 3 provide a visual representation of the chemically active sites and comparative reactivity of the atoms.

HOMO–LUMO analysis

HOMO and LUMO are very important parameters for quantum chemistry. We can determine the way the molecule interacts with other species; hence, they are called the frontier orbital. HOMO can be thought as the outermost orbital containing electron, which is ready to give these electrons and hence can act as an electron donor [21]. On the other hand, LUMO can be thought as the innermost orbital containing free places to accept electrons and hence acts as an electron
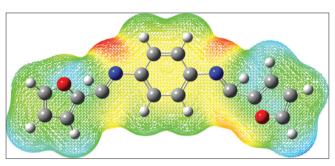
acceptor. The gap between HOMO and LUMO characterizes molecular chemical stability. The frontier orbital gap helps to identify the chemical reactivity and kinetic stability of the molecule. A molecule with a small frontier orbital gap is more polarizable and is generally associated with high chemical reactivity, low kinetic stability and is also termed as soft molecule. The lower value of frontier orbital gap in case of the title compound makes it more reactive and less stable.

The HOMO and LUMO energy of the compounds are calculated by B3LYP method using 6-31 G(d) basic set. This electronic transition absorption corresponds to the transition from the ground to the first excited state and is mainly described by an electron excitation from the HOMO to the LUMO. In compound **3**, the HOMO is located over the furan and imino group the HOMO → LUMO transition implies an electron density transfer to the entire ring. The atomic compositions of the frontier molecular orbital are shown in Fig. 4. The calculated self-consistent field energy for the title compound is −870.6290 atomic units (a.u.). The energy gap between HOMO and LUMO explains the eventual charge transfer interaction within the molecule. The frontier orbital energy gap is found to be 0.25235 a.u. The narrow energy gap between HOMO and LUMO facilitates intramolecular charge transfer which makes the material to be NLO active.

This electronic absorption corresponds to the transition from the ground to the first excited state and is mainly described by one electron
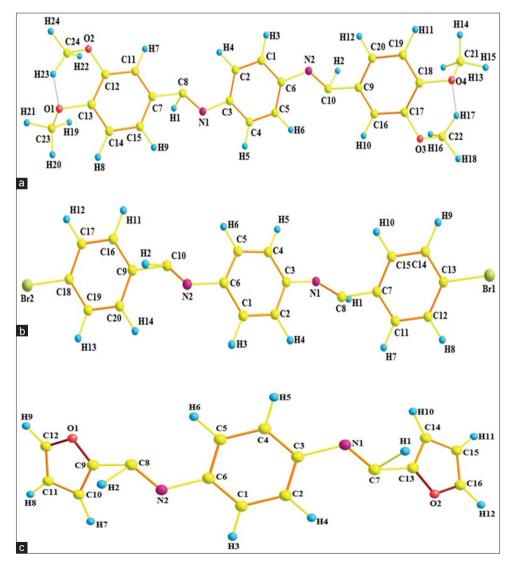

Fig. 2: Molecular electrostatic potential map of the compound 3

Fig. 3: Optimized structure of the compounds 1-3 (a–c)

excitation from the HOMO to the LUMO. Many organic molecules containing conjugated π electron are characterized by large value of molecular first hyper polarizabilities and were analyzed by means of vibrational spectroscopy. In most of the cases, even in the absence of inversion symmetry, the strongest band in the Raman spectrum is weak in the IR spectrum and vice versa. However, the intramolecular charge from the donor to acceptor group through a single-double band conjugated path can induce large variations of both the molecular dipole moment and the molecular polarizability, making IR, and Raman activity strong at the same time. The experimental spectroscopic behavior described above is well accounted for DFT calculations in π conjugated system that predict exceptionally infrared intensities for the same normal modes.

NLO properties

The first hyperpolarizability (β), dipole moment (μ), and polarizability (α) are calculated using B3LYP/6-311++G(d, p) basis set on the basis of the finite-field approach [22]. The complete equations for calculating the magnitude of total static dipole moment μ, the mean polarizability α_0, the anisotropy of the polarizability <α>, and the first polarizability β_0, using the *x*, *y*, and *z* components from Gaussian 03W output are as follows:

$$a_0 = \frac{a_{xx}a_{yy}a_{zz}}{3} \tag{1}$$

$$a = 2^{-1/2}[(a_{xx}-a_{yy})^2 + (a_{yy}-a_{zz})^2 + a_{zz}-a_{xx})^2 + 6\,a_{xx}{}^2]^{1/2} \tag{2}$$

$$\beta_0 = (\beta^2x + \beta^2y + \beta^2z)^{1/2} \tag{3}$$

$$\beta_x = \beta_{xxx} + \beta_{xyy} + \beta_{xzz} \tag{4}$$

$$\beta_y = \beta_{yyy} + \beta_{xxy} + \beta_{yzz} \tag{5}$$

$$\beta_z = \beta_{zzz} + \beta_{xxz} + \beta_{yyz} \tag{6}$$

In Table 1, the calculated parameters described above and electronic dipole moment {μ_i (*i* = *x*, *y*, *z*) and total dipole moment μ_{tot}} for the title compound are listed. The total dipole moment can be calculated using the following equation:

$$\mu = (\mu^2x + \mu^2y + \mu^2z)^{1/2} \tag{7}$$

It is well known that the higher values of dipole moment, molecular polarizability, and hyperpolarizability are responsible for NLO properties [23]. The polarizabilities and hyperpolarizability are reported in a.u, the calculated values have been converted into electrostatic units (esu) (for α; 1 a.u = 0.1482×10^{-24} esu and for β; 1 a.u = 8.6393×10^{-33} esu) (Tables 1 and 2). The calculated value of dipole moment (μ) was found to be 2.0451. The highest value of dipole moment is observed for component μ_x. In this direction, this value is equal to 1.4828 D. The calculated polarizability and anisotropy of the polarizability are 119.7906 esu. The magnitude of the molecular hyperpolarizability β is one of the important key factors in a NLO system. The B3LYP calculated first hyperpolarizability value (β) is equal to 7.14767×10^{-31} esu [24]. The dipole moment and first hyperpolarizability indicate that the compound **1** has NLO properties and it is approximately 1.48929 and 1.9168307×10^{-60} times than those of urea.

Mulliken charges

The calculation of atomic charges plays an important role in the application of quantum mechanical calculation to molecular systems [25-27]. The charge distributions of the compound **3** have been calculated by B3LYP/6-31G (d) method. The magnitude of the carbon atomic charges is found to be either positive or negative and is noted to change from −0.506530 to 0.240473. It is also evident from the table that H39 has the maximum positive charge (0.248220) and hence it acts as an acceptor atom. N8 has maximum negative charge (−0.565019) and
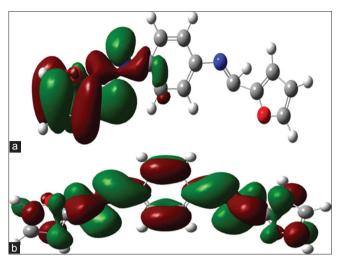

Fig. 4: Highest occupied molecular orbital (a) and lowest unoccupied molecular orbital (b) of the compound 3

Table 1: The electric dipole moment μ (D) the average polarizability α_{tot} and the first hyperpolarizability

Parameters	Value	Parameters	Value
μ_x	1.4828	β_{xxx}	76.0572
μ_y	−1.3332	β_{xxy}	−57.5488
μ_z	0.4541	β_{xyy}	10.9644
M	2.0451	β_{yyy}	−10.0294
α_{xx}	−60.5716	β_{xxz}	45.7268
α_{xy}	2.6148	β_{xyz}	−9.4778
α_{yy}	−111.5277	β_{yyz}	2.4459
α_{xz}	1.8511	β_{xzz}	−5.0716
α_{yz}	1.8954	β_{yzz}	−0.9673
α_{zz}	−122.1051	β_{zzz}	2.8393
α_{tot} (esu)	119.7906	β_{tot} (esu)	7.14767

esu: Electrostatic units

Table 2: Calculated thermodynamic parameters employing B3LYP using 6−31G(d) basis set

Thermodynamic parameters (298 K)	DFT/6−311 g++(d,p)
SCF energies (a.u.)	−870.6290966
HOMO-LUMO gap ev	0.25235
Chemical potential μKJ/mol	0.154015
Global hardness ηKJ/mol	−0.126175
Electronegativity χ KJ/mol	0.154015
Global softness S KJ/mol	−3.9447731
Electrophilicity index ωKJ/mol	−0.093999
Rotational constants (GHz)	
A	0.50146
B	0.04968
C	0.04524

SCF: Self-consistent field, HOMO-LUMO: Highest occupied molecular orbital–lowest unoccupied molecular orbital, DFT: Density functional theory, a.u: Atomic units

it acts as donor atom. The above result shows that the natural atomic charges are more sensitive to the changes in the molecular structure than Mulliken's net charges.

In vitro antibacterial activity

All of our synthesized compounds (**1-3**) were tested for their antimicrobial activity against two test organisms, namely *S. aureus* and *E. coli*. The agar well-diffusion method was used for studying the potential activities of these compounds. Streptomycin used as a positive

control. The activity results of our synthesized compounds against *S. aureus* and *E. coli* are shown in Table 3, as the zone of inhibition (in mm). The photographs showing that the zone of inhibition of the tested compounds against the different microorganisms is given in Fig. 5. The compound **1** exhibits significant antibacterial activity compared to standard drug streptomycin against tested organism. The potential antibacterial activity of compounds may be due to the increase in lipophilicity and affects the partitioning of molecules into membranes and facilitates hydrophobic interactions of the molecules with specific binding sites on either receptor or enzymes. Analysis of the data in Table 3 reveals that all the synthesized compounds showed good antimicrobial activity when tested against antibacterial strains such as *S. aureus* and *E. coli.*

In silico studies

Molecular docking with antibacterial protein beta-ketoacyl-acp synthase III

Based on the antibacterial results, all the compounds have showed significant antibacterial activity when compared to standard drug. This prompted us, to do molecular docking studies with compounds against antibacterial protein beta-ketoacyl-acp synthase III (PDB: 1HNJ). All the compounds (**1-3**) are effectively interacted with the active sites of beta-ketoacyl-acp synthase III through π–π, σ–π, hydrogen bonding, electrostatic, and Van der Waals interactions (Fig. 6) and the binding energy values are noted in Table 4. The compound **1** shows two π–π interaction, first one was formed between the 3,4-dimethoxybenzene ring and LEU 189 (bond length: 3.5 Å) and second one was formed between another 3,4-dimethoxybenzene ring and HIS 244 (bond length: 3.7 Å). The compound **1** was stabilized by four hydrogen bonding interaction, first one was formed between hydrogen atom of ALA 111 and oxygen atom (–O) of the 3,4-dimethoxybenzene ring (bond length: H···O=3.8 Å), second one was formed between hydrogen atom of LEU 205 and oxygen atom (–O) of the 3,4-dimethoxybenzene ring (bond length: H···O=4.1 Å), third one was formed between hydrogen atom of ILE 250 and oxygen atom of –O of the 3,4-dimethoxybenzene ring (bond length: H···O=4.6 Å), and fourth one was formed between hydrogen atom of GLY 305 and nitrogen atom of (–N) the (1,4-phenylene) dimethanimine present in the compound (bond length: H···N=2.5 Å). Moreover, the binding model was enhanced by electrostatic interaction formed between compound **1** and residues CYS 112, PHE 304, GLU 302, HIS 244, and ILE 251, and Van der Waals interaction formed between compound **1** and residues LEU 205, THR 281, LEU 191, THR 190, ALA 111, LEU 189, GLY 306, ALA 303, LEU 220, PRO 243, THR 254, ILE 250, ASN 247, ALA 246, ASN 274, and LEU 142 of beta-ketoacyl-acp synthase III receptor [28-30].

The compound **2** shows one σ–π interaction formed between the 3,4-dimethoxybenzene ring and ILE 250 (bond length: 3.8 Å), which also stabilized by two hydrogen bonding interaction, first one was formed between hydrogen atom of LEU 220 and bromine atom (–Br) of the 4-bromobenzene ring (bond length: H···Br = 3.1 Å) and second one was formed between hydrogen atom of ALA 246 and nitrogen atom of –N the (1,4-phenylene) dimethanimine present in the compound (bond length: H···N = 4.6 Å). Moreover, the binding model was enhanced by electrostatic interaction formed between compound **2** and residues CYS 112, PHE 304, GLY306, HIS 244, and ILE 251, and Van der Waals interaction formed between compound **2** and residues GLU 302, PRO 243, LEU 220, ILE 250, ASN 247, ALA 246, ASN 274, LEU 189, LEU 191, LEU 142, THR 81, ALA 11, and GLY 305 of beta-ketoacyl-acp synthase III receptor.

The compound **3** shows two π–π interaction; the first one was formed between the furan ring and HIS 244 (bond length: 3.6 Å) and the second one was formed between the phenyl ring and HIS 244 (bond length: 3.5 Å). The compound **3** was stabilized by two hydrogen bonding interaction, first one was formed between hydrogen atom of HIS 244 and oxygen atom (–O) of the furan ring (bond length: H···O = 3.2 Å) and second one was formed between hydrogen atom of CYS 112 and nitrogen of –N the (1,4-phenylene)dimethanimine present in the

Fig. 5: Zone of inhibition of compounds (1-3) against bacterial strain *Staphylococcus aureus* and *Escherichia coli*
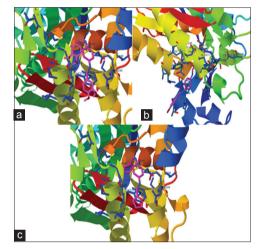

Fig. 6: Docked result showing the interaction between active site residues of beta-ketoacyl-acp synthase III, and compounds 1 (a), 2 (b), and 3 (c)

Table 3: Antibacterial activity of synthesized compounds (1-3)

Compounds	Zone of inhibition (mm)	
	Staphylococcus aureus	*Escherichia coli*
1	16	18
2	11	13
3	9	10
Streptomycin	13	15

compound (bond length: H···N = 4.3 Å). Moreover, the binding model was enhanced by electrostatic interaction formed between compound **3** and residues GLY 306, CYS 112, PHE 304, and HIS 244, and Van der Waals interaction formed between compound **3** and residues LEU 142, LEU 191, LEU 205, ALA 246, ALA 303, LEU 220, ILE 250, GLY 305, ASN 234, LEU 189, and PHE 157 of beta-ketoacyl-acp synthase III receptor.

Molecular docking with anticancer protein c-Kit tyrosine kinase receptor

The synthesized compounds were also docked with anticancer protein c-Kit tyrosine kinase with (PDB: 1t46). The analysis of the results show all the compounds interacted with enzyme c-Kit tyrosine kinase through π–π, σ–π, hydrogen bonding, electrostatic, and Van der Waals interactions (Fig. 7). The compound **1** shows two π–π interaction, first one was formed between the 3,4-dimethoxybenzene ring and LYS 623 (bond length: 3.6 Å) and second one was formed between the (1,4-phenylene) dimethanimine ring and HIS 790 (bond length: 3.5 Å), which also shows one σ–π interaction formed between the 3-methoxy group present in the 3,4-dimethoxybenzene ring and PHE 811 (bond length: 3.4 Å). The compound **1** was stabilized by four hydrogen

Table 4: Result of docking studies between beta-ketoacyl-acp synthase III + malonyl-CoA receptor (PDB: 1HNJ) with compounds

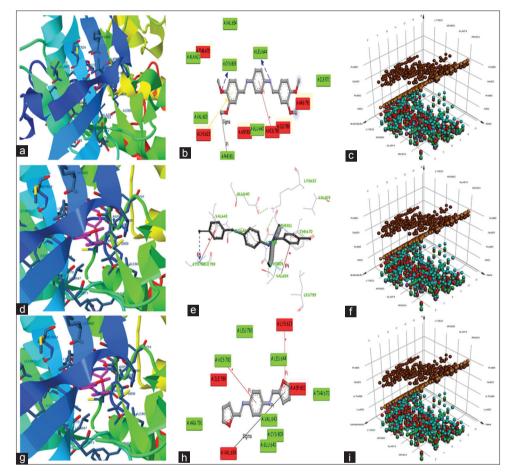| S. No.	Est. Free energy of binding (kcal/mol)	Est. inhibition constant (uM)	vdW + Hbond + desolv energy (kcal/mol)	Electrostatic energy (kcal/mol)	Total intermolec energy (kcal/mol)	Interact. surface
beta-ketoacyl-acp synthase III + malonyl-CoA receptor						
1	−6.24	26.88	−7.35	−0.05	−7.41	706.614
2	−4.69	364.96	−6.99	−0.05	−7.03	864.148
3	−4.80	304.38	−5.67	−0.24	−5.90	699.788
c-Kit tyrosine kinase receptor						
1	−8.04	1.27	−9.20	−0.02	−9.22	839.019
2	−7.50	3.17	−9.45	−0.21	−9.67	993.158
3	−6.73	11.70	−7.63	−0.11	−7.74	713.581

Fig. 7: Docked result showing the interaction between active site residues of c-Kit tyrosine kinase and compounds 1 (a–c), 2 (d–f), and 3 (g–i)

bonding interaction, first one was formed between hydrogen atom of ARG 791 and oxygen atom (–O) of the 3,4-dimethoxybenzene ring (bond length: H···O = 3.6 Å), second one was formed between hydrogen atom of CYS 809 and oxygen atom (–O) of the 3,4-dimethoxybenzene ring (bond length: H···O = 4.0 Å) and third one was formed between hydrogen atom of LEU 644 and nitrogen atom of (–N) the (1,4-phenylene) dimethanimine present in the compound (bond length: H···N = 3.9 Å). Moreover, the binding model was enhanced by electrostatic interaction formed between compound **1** and residues THR 670, LYS 623, ASP 810, HIS 790, ILE 789, and ARG 791, and Van der Waals interaction formed between compound **1** and residues PHE 811, VAL 603, ALA 621, CYS 809, VAL 654, LEU 644, GLU 640, and ILE 571 of c-Kit tyrosine kinase.

The compound **2** shows two π–π interaction; first one was formed between the 4-bromobenzene ring and VAL 654 (bond length: 3.7 Å) and second one was formed between the 4-bromobenzene ring and CYS 788 (bond length: 3.6 Å). The compound **2** was stabilized by two hydrogen bonding interaction, first one was formed between hydrogen

atom of CYS 788 and bromine atom (–Br) of the 4-bromobenzene ring (bond length: H···O = 3.9 Å) and second one was formed between hydrogen atom of PHE 811 and bromine atom (–Br) of the 4-bromobenzene ring (bond length: H···O = 4.7 Å). Moreover, the binding model was enhanced by electrostatic interaction formed between compound **2** and residues THR 670, ASP 810, LYS 623, ILE 789, PHE 811, and GLU640, and Van der Waals interaction formed between compound **2** and residues LEU 644, VAL 647, LYS 785, VAL 603, CYS 809, LEU 799, and VAL 654 of c-Kit tyrosine kinase.

The compound **3** shows two π–π interaction, first one was formed between the furan ring and LYS 623 (bond length: 3.7 Å) and second one was formed between the (1,4-phenylene) dimethanimine ring and HIS 790 (bond length: 3.6 Å), which also shows one σ–π interaction formed between the 3-methoxy group present in the furan ring and VAL 654 (bond length: 3.5 Å). The compound **3** was stabilized by one hydrogen bonding interaction, formed between the hydrogen atom of ASP 810 and oxygen atom (–O) of the furan ring (bond length: H···O = 3.8 Å).

Moreover, the binding model was enhanced by electrostatic interaction formed between compound **3** and residues ILE 789, LYS 623, and ASP 810, and Van der Waals interaction formed between compound **3** and residues ARG 791, VAL 654, VAL 647, CYS 809, GLU 640, LEU 644, LEU 783, HIS 790, and THR 670 of c-Kit tyrosine kinase.

The observed data clearly indicate both beta -ketoacyl-acp synthase III and c-Kit tyrosine kinase receptor as the effective inhibitor for all the compounds. Among the compounds, the compound **1** strongly binds with both beta-ketoacyl-acp synthase III as well as c-Kit tyrosine kinase receptor, then the other compounds, this is consistent with the above antibacterial studies.

CONCLUSION

In this study, heterocyclic Schiff bases compounds (**1-3**) have been synthesized and characterized by analytical methods. The calculated HOMO and LUMO energies show the high chemical reactivity of the molecules and support the high bioactivity of the compounds. The first-order hyperpolarizability results indicate that the compounds are a good activity of NLO property. *In vitro* antibacterial activity revealed that the compounds (**1-3**) possess potent antibacterial activities toward bacteria and compound **3** shows potent activity compared to standard drug streptomycin. The molecular docking results showed that the compounds strongly interact with both antibacterial and anticancer receptor protein and gives better free energy of bindings.

CONFLICTS OF INTEREST

The authors declare that they have no conflicts of interest.

REFERENCES

1. Zhang X, Wang H, Li Y, Cao R, Zhong W, Zheng Z, *et al.* Novel substituted heteroaromatic piperazine and piperidine derivatives as inhibitors of human enterovirus 71 and coxsackievirus a16. Molecules 2013;18:5059-71.
2. Vitaku E, Smith DT, Njardarson JT. Analysis of the structural diversity, substitution patterns, and frequency of nitrogen heterocycles among U.S. FDA approved pharmaceuticals. J Med Chem 2014;57:10257-74.
3. Cimerman Z, Miljanic S, Galic N. Schiff bases derived from aminopyridines as spectrofluorimetric analytical reagents. Croat Chem Acta 2000;73:81-95.
4. Singh P, Goel RL, Singh BP. 8-acetyl-7-hydroxy-4-methyl coumarin as a gravimetric reagent for Cu^{2+} and Fe^{3+}. J Indian Chem Soc 1975;52:958-9.
5. Elmali A, Kabak M, Elerman Y. Keto–enol tautomerism, conformations and structure of N-(2-hydroxy-5-methylphenyl), 2-hydroxybenzaldehydeimine. J Mol Struct 2000;477:151-8.
6. Patel PR, Thaker BT, Zele S. Preparation and characterization of some lanthanide complexes involving a heterocyclic$_\beta$-diketone. Indian J Chem 1999;38A:563-7.
7. Berry BF, Beezer AE, Miles RJ, Smith BW, Miller J, Nascimento MG. Evaluation of microcalorimetry as a drug bioactivity screening procedure: application to a series of novel schiff base compounds. Microbois 1988;45:181.
8. Lawrence JF, Frei RW. Chemical Derivatization in Chromatography. Amsterdam: Elsevier; 1976.
9. Thilagavathi R, Kavitha HP, Arulmozhi R, Babu SM. Synthesis of 3-{4-[4-(benzylideneamino) benzene sulfonyl]-phenyl}-2-phenylquinazoline-4(3H)-one. Molbank 2009;M589:1-3.
10. Sain B, Sandhu JS. An efficient one-pot synthesis of 1,3,4-oxadiazoles and 4H-3,1-benzoxazin-4-ones. Indian J Chem 1992;31:768-70.
11. Guo Z, Xing R, Liu S, Zhong Z, Xi J, Wang L. Antifungal properties of Schiff bases of chitossan, N-substituted chitosan and quaternized chitosan. Carbohydr Res 2007;342:1329-32.
12. Ahmed I, Beg AJ. Antimicrobial and phytochemical studies on 45 Indian plants against multi-drug resistant human pathogens. J Enthnopharmacol 2001;74:113-23.
13. Bikadi Z, Hazai E. Application of the PM6 semi-empirical method to modeling proteins enhances docking accuracy of autodock. J Cheminform 2009;1:15-20.
14. Halgren TA. Merck molecular force field. I. Basis, form, scope, parameterization, and performance of MMFF94. J Comput Chem 1998;17:490-519.
15. Morris GM, Goodsell DS, Halliday RS, Huey R, Hart WE, Belew RK, *et al.* Automated docking using a lamarckian genetic algorithm and an empirical binding free energy function. J Comput Chem 1998;19:1639-62.
16. Solis FJ, Wets RJ. Minimization by random search techniques. Math Oper Res 1981;6:19-30.
17. Raman N, Thangaraja C. Synthesis and structural characterization of a fully conjugated macro-cyclic tetra-aza chiral schiff –bases. Trans Met Chem 2005;30:317-22.
18. Sabah HH. Synthesis, spectroscopic characterization of schiff bases derived from 4,4'-methlendianiline. Pharm Chem 2014;6:38-41.
19. Uludag N, Serdaroglu G. An improved synthesis (FT-IR, NMR) study and DFT computational analysis (IR, NMR, UV-Vis, MEP diagrams, NBO, NLO, FMO) of the 1,5-methanoazocino [4,3-b] indole core structure. J Mol Struct 2018;1155:548-60.
20. Kavitha T, Velraj G. Molecular structure, spectroscopic and docking analysis of 1,3-diphenylpyrazole-4-propionic acid: A good prostaglandin reductase inhibitor. J Mol Struct 2018;1155:819-30.
21. Karabacak M, Cinar Z, Cinar M. Structural and spectroscopic characterization of 2,3-difluorobenzoic acid and 2,4-difluorobenzoic acid with experimental techniques and quantum chemical calculations. Spectrochim Acta Part A 2011;79:1511-9.
22. Prashanth J, Reddy BV. Study on structure, vibrational analysis and molecular characteristics of some halogen substituted azido-phenylethanones using FTIR spectra and DFT. J Mol Struct 2018;1155:582-97.
23. Eşme A, Sağdınç SG. Spectroscopic (FT-IR, FT-Raman, UV-Vis) analysis conformational, HOMO-LUMO, NBO and NLO calculations on monomeric and dimeric structures of 4-pyridazinecarboxylic acid by HF and DFT methods. J Mol Struct 2017;1147:322-34.
24. Oliveira BG, Duarte EM, Araújo RC, Ramos MN, Carvalho AB. A theoretical study of nonlinearity in heterocyclic hydrogen-bonded complexes. Spectrochim Acta Part A 2005;61:491-4.
25. Rahmani R, Boukabcha N, Chouaih A, Hamzaoui F, Goumri-Said S. On the molecular structure, vibrational spectra, HOMO-LUMO, molecular electrostatic potential, UV-Vis, first order hyperpolarizability, and thermodynamic investigations of 3-(4-chlorophenyl)-1-(1yridine-3-yl) prop-2-en-1-one by quantum chemistry calculations. J Mol Struct 2018;1155:484-95.
26. Rajan TS, Aanandhi MV. Molecular docking studies of isolated flavonoids compounds from *Amaranthus tristis* Linn. As alpha-amylase and alpha-glucosidase activators. Asian J Pharm Clin Res 2018;10:62-5.
27. Mohanambal D, Arulantony S. Synthesis, characterization of schiff base complexes based on pyrimidine moiety with molecular docking with biomolecules. Asian J Pharm Clin Res 2018;10:93-7.
28. Patel KM, Chaudagari KK, Mehta AA. Role of nitric oxide (NO) in capsaicin mediated anti-platelet activity in *in vitro*, *in vivo*, *ex-vivo* model of platelet aggregation assay and arterial thrombosis in rat: Potential therapeutic target? Int J Pharm Pharm Sci 2018;10:44-8.
29. Miladiyah I, Jumina J, Haryana SM, Mustofa M. *In silico* molecular docking of xanthone derivatives as cyclooxygenase-2-inhibitor agents. Int J Pharm Pharm Sci 2017;9:98-104.
30. Pradeep PS, Kumar TO, Prashantha N, Mahadevan KM. Syntheis, *in vitro* antibacterial, toxicity and molecular docking anticancer activity of novel N-[(2-Chloroquinolin-3-yl)Methylidene]-2-aniline schiff bases. Int J Curr Pharm Res 2015;7:37-46.